UNIVERSIDADE FEDERAL DE LAVRAS

OTÁVIO CASTRO MENDONÇA

A DINÂMICA TEMPORAL DA REORIENTAÇÃO DO OLHAR
NA CORUJA CABURÉ

LAVRAS - MG
2021

OTÁVIO CASTRO MENDONÇA

A DINÂMICA TEMPORAL DA REORIENTAÇÃO DO OLHAR NA CORUJA CABURÉ

<div align="right">

Monografia apresentada à Universidade Federal de Lavras, como parte das exigências do Curso de Ciências Biológicas, para a obtenção do título de Bacharel.

</div>

Prof. Dr. Jerome Paul Armand Laurent Baron

Orientador

LAVRAS - MG
2021

OTÁVIO CASTRO MENDONÇA

A DINÂMICA TEMPORAL DA REORIENTAÇÃO DO OLHAR NA CORUJA CABURÉ
TEMPORAL DYNAMICS OF VISUAL GAZE SHIFTS IN THE FERRUGINOUS PYGMY OWL

> Monografia apresentada à Universidade Federal de Lavras, como parte das exigências do Curso de Ciências Biológicas, para a obtenção do título de Bacharel.

Aprovada em: 29 / 11 / 2021

Prof. Dr. Jerome Paul Armand Laurent Baron UFMG
Prof. Dr. Theo Rolla Motta UFMG
Profa. Dra. Danielle Oliveira Costa Santos UFSB

_____
Prof. Dr. Jerome Paul Armand Laurent Baron

Orientador

LAVRAS - MG
2021

Aos meus pais, Ronaldo e Imaculada.

AGRADECIMENTOS

O presente trabalho foi desenvolvido no formato de artigo e atualmente encontra-se a ser

submetido à revista Animal Behaviour.

Temporal dynamics of visual gaze shifts in the Ferruginous pygmy owl

Otávio Mendonça [1], Cíntia Aparecida de Souza Garcia[3], Alice Timponi França[3], Jerome Baron [2 CA]

[1] Undergraduate in Biological Sciences, Federal University of Lavras, 37200-900, Lavras, Brazil

[2] Department of Physiology and Biophysics, Institute of Biological Sciences, Federal University of Minas Gerais, 31270-901 Belo Horizonte, Brazil

[3] Graduate in Physiology and Biophysics, Institute of Biological Sciences, Federal University of Minas Gerais, 31270-901 Belo Horizonte, Brazil

Corresponding author: Jerome Baron

Number of words for Abstract 142

Number of words for Introduction 471

Number of words for Methods 1 094

Number of words for Results 738

Number of words for Discussion 1 121

Conflict of Interest: The authors declare no competing financial interests.

Correspondence: jbaron@ufmg.br

ABSTRACT

Saccade temporal dynamics dictate when vertebrates will shift their gaze. These movements constitute the main visual sampling mechanism in this group. It is shown that their presence deeply modulates activity in primary visual areas increasing sensory information extraction. However, probabilistic neurophysiological models related to visual perception often require experimental conditions in which these events are partially or totally restricted. In this sense, contemporary models must incorporate the visuomotor temporal patterns of unrestrained subjects in order to satisfactorily explain this sensory domain. Here we characterized Ferruginous pygmy owl saccade temporal dynamics in a naturalistic setting using a mathematical method introduced for characterizing activity fluctuations of complex systems. By analysing video recordings we found that in this species saccades temporal dynamics display a bursty pattern. This approach permitted practical comparison with other primate and owl species providing a comparative perspective of this behaviour.

Keywords: saccadic gaze shifts, owls, temporal dynamics, Memory coefficient, Burstiness index.

HIGHLIGHTS

This is the first study applying Goth and Barabasi (2008) mathematical method for characterizing saccade temporal dynamics. Also represents one the first attempts to quantitatively characterize saccade temporal dynamics in a avian species.

INTRODUCTION

Vertebrates exhibit a variety of visuomotor scanning strategies for effectively acquiring visual sensory information (Land 2019). In this group, vision is an active process that depends on the rapid alignment of areas of higher visual acuity in the retina to salient objects in a scene (Land 2015). They do so by performing saccadic gaze shifts, or saccades, that depending on the species or experimental setting may emerge as a result of independent or conjugate eye, head and/or body movements (Hayhoe 2005, Yorzinski 2015).

During the course of saccades, high retinal velocities combined with the long response time of the photoreceptors results in significant image degradation (Land 1999). On the other hand, not only their presence but also the particular timing in which these movements occur may be essential for the effective extraction of visual sensory information through an increase in the signal-to-noise ratio in neurons in primary visual areas (Baudot 2013). Therefore the temporal structure of saccade occurrences must be governed by a cost-effective optimization principle. Considering this, in any attempt to model the neurophysiology of visual perception not only the spatial but also the temporal dimension of saccades must be taken into account.

Owls are important well-established animal models in the study of sensory perception (Wagner 2013). Several discoveries concerning this avian group's visual processing and visuomotor behaviour indicated apparent evolutionary convergences with primates (Baron 2007, Pinto 2009, Ohayon 2006). Despite the similarities, because owls eyes are almost completely immobile this bird visual search is mainly constituted by head saccades. This feature facilitates detection and makes it possible to identify gaze shifts in a video recording of a freely behaving animal.

In this study, we investigated the saccades temporal proprieties of the Ferruginous pygmy owl, a minute generalist predator widely distributed in the Americas (Sarasola 2014, Cartron 2000). In contrast with barn owls (*Tyto alba*), the most usual owl animal model in literature this species is active during the day (Sazima 2015, Motta-Junior 2007). This activity pattern indicates the presence of adaptations to daylight conditions like a better defined high-resolution area in the retina or real fovea which better resemble the one of a primate.

We characterize the saccade temporal dynamics of Ferruginous pygmy owls in a naturalistic setting using a method introduced by Goth and Barabasi (2008) following a prospective visual inspection of the saccade time series and instantaneous saccade rate which indicated the presence of short periods with a sudden activity increase resulting in saccade clusters. Through the assessment of the two orthogonal measures, this mathematical approach has been widely used to characterize and compare activity fluctuations of diverse complex systems ranging from earthquakes to physiological processes such as heartbeats (Goh 2008).

We found that saccadic gaze shifts in Ferruginous pygmy owls display a intermitente or bursty activity pattern what means they present periods with rapid increases in the saccade rate followed by periods of diminished activity. Comparisons with saccade sequences from other vertebrate species including humans show detectible inter-species differences offering an opportunity to investigate the temporal dynamics of saccades from a comparative point of view.

METHODS

Animals and Recording Setup

Four Ferruginous pygmy owls (*Glaucidium brasilianum;* designated as GB1902, GB1903, GB1904, GB1905*)* were obtained from the Brazilian Institute of the Environment and Renewable Natural Resources (IBAMA/IEF) and maintained for scientific purposes under the license no. 3076223. Using a SONY Handycam (https://handykam.com) infra-red câmera (25 Hz sampling frequency) the birds were filmed behaving freely in a 30 x 60 x 20 cm cage exposed to natural light to which they were previously habituated near the Institute of Biological Sciences of the Federal University of Minas Gerais (UFMG). To prevent interference by great central state transitions the videos were recorded between 12:00 and 13:00 (1 hour) in the course of nine days in May 2019. During this period they were individually placed All experimental procedures were approved by the UFMG's Ethics Committee for Animal Experimentation (CETEA, license no. 2004/01).

Video Analyses

The video recordings were analyzed through frame-by-frame manual behavioural coding with 40 ms precision using the software BORIS (https://boris.readthedocs.io). In order to visually scan their surroundings, owls perform a complex combination of head movements that have either a predominant rotational (saccade) or translational component (peering) (Ohayon 2006). These two types of head movements were easily distinguished in the videos and the occurrence of head saccades as well as several other identified behaviours extracted as time series. Descriptions of the codded behaviours are presented in a etogram (Table 1).

Table 1. Etogram.

Behaviour	Description
Saccade	Rapid gaze shift with a strong rotational component (Ohayon 2006) as a result of neck and head movement in relation to the animal's torso. Occasionally accompanied by a monocular or binocular blink (see blink description).
Peering	Head movement with a strong translational component (Ohayon 2006) in both the horizontal and vertical planes accompanied by neck and occasionally torso movement during which the animal apparently maintain the skull in a fixed orientation.
Smooth pursuit	Long-lasting, low-speed head movements (greater than 500ms) as a result of mainly neck movement. Usually performed when the animal follows moving objects. Both eyes remain open.
Blink	Rapid closure of one or both eyes immediately followed by reopening of one or both eyes, during which the animal keeps its head fixed.
Locomotion	Animal jump, fly or walk in the cage.
Maintenance	Animal performs cleaning, feather maintenance or lengthens legs and wings.
Drowsiness	Prolonged immobility with a relaxed neck. It may be accompanied by resting the head on one of the wings. When visible, one or both eyes can be open, partially open or closed for more than 1000ms.

As a consequence of the 40 ms temporal resolution, ISIs with less than 80 ms (1 frame interval) were considered as a single saccade interval. For subsequent analyses, a discrete signal representing saccade occurrences was obtained by extracting the onset time of each saccade. Then the instantaneous saccade rate (ISR) were calculated as:

$$ISR_n = \frac{\beta}{t_n - t_{n-1}}$$

Where t_n is the saccade onset times in milliseconds and $\beta = 1\ 000$ since the ISR is expressed in saccades per second.

Model fitting and model selection

Several analytical approaches can be used to characterize the temporal patterns of head saccades. Initially, we prospectively analyzed our data by assessing how well the ISI distribution could be described by distinct probability distribution functions often considered in the primate eye-movement literature. We considered 4 possible models.

First, we checked whether saccade events were randomly distributed in time according to a simple (one parameter) homogeneous Poisson model. The assumption of this model is that the exact time of each saccade is random but the mean interval between saccades is constant. The distribution of such a sequence follows an exponential distribution mathematically described as:

$$f(ISI_n; \lambda) = \frac{1}{\lambda} exp\left(\frac{-ISI_n}{\lambda}\right)$$

where the average number of events per unit of time (rate) is a constant defined by $\frac{1}{\lambda}$.

However, it is reasonable to assume that the process underlying the triggering of a next saccade may not be entirely random. Many studies in the human and non-human primate literature have shown that a saccade can not be visually triggered at the beginning of a fixation, a period known as a post-saccadic "refractory period". Presumably, this period is explained by the neural signal conduction time linking visual processing to saccade generator centers. On theoretical grounds, Harris (1989) argued that if one incorporates this constraint in a framework whereby saccades are triggered by multiple visual targets of equal saliency and

probabilistically appearing in time, the resulting occurrence of saccades will show a first-order dependency of ISIs satisfactorily captured by a Weibull distribution defined as:

$$f(ISI_n; \alpha, \beta) = \frac{\beta}{\alpha} \left(\frac{ISI_n}{\alpha}\right)^{\beta-1} exp\left[-\left(\frac{ISI_n}{\alpha}\right)^{\beta}\right]$$

where the free parameters α and β represent the scale and shape parameters, respectively. When $\beta = 0$, the process assumes an exponential decay. When $\beta < 1$ and $\beta > 1$, the decay rate decrease or increase, respectively.

In human subjects freely watching movie clips, a condition close to ours in terms of visual immersion, Wang et al. (2012) found a consistent temporal deployment of eye saccades well predicted by a log-normal distribution model given by:

$$f(ISI_n; \mu, \sigma) = \frac{1}{ISI_n \alpha \sqrt{2\pi}} exp\left[-\left(\frac{log(ISI_n) - \mu}{2\alpha^2}\right)^2\right]$$

In this model, the scale and shape parameters are defined by σ and μ, respectively. We also fit our data with a Sinh-arcsinh (SHASH) distribution, a four-parameter model defined as:

$$f(ISI_n \mid \mu, \sigma, \epsilon, \delta) = \frac{\delta cosh(\omega)}{\sqrt{\sigma^2 + (ISI_n - \theta)^2}} \phi[sinh(\omega)]$$

where $\phi(.)$ is the standard normal probability, and:

$$\omega = \epsilon + sinh^{-1}\left(\frac{ISI_n - \theta}{\sigma}\right)$$

The parameters θ, σ, ϵ and δ correspond to the location (central tendency), scaling (standard deviation), skewness and kurtosis of the distribution. Positive (negative) skewness is evidenced when $\epsilon > 0$ ($\epsilon < 0$). Interestingly, when $\epsilon = 0$ and $\delta = 1$, the SHASH model corresponds to a normal distribution with mean and standard deviation equal to θ and σ. Distributions with heavier (lighter) tails than a normal distribution have $\delta < 1$ ($\delta > 1$).

To assess the relative performance of each fitted model, we used a model selection approach based on the Akaike information criterion (AIC; Akaike, 1974). Detailed information about the theoretical concepts and mathematical formalisms underlying this information criterion are provided in Burnham and Anderson (2002). Because AIC values vary on a relative scale and are much affected by the data sample size, we used their differences to the minimal value min(AIC) within the model set under consideration defined as:

$$\Delta AIC_c^i = AIC_c^i - min(AIC_c)$$

Burstiness and Memory quantification

In order to better characterize the temporal structure of saccade sequences, we used a simple yet robust mathematical method effectively applied for characterizing activity

fluctuations in complex systems introduced in (Goh 2008). Following this method, we quantify two metrics. First, the burstiness index (B), defined as:

$$B = \frac{\sigma_i - \langle \tau_i \rangle}{\sigma_i + \langle \tau_i \rangle}$$

B is a distribution based measure defined as time scale normalized form of the coefficient of variation where $\langle \tau_i \rangle$ is the mean and σ_i is the standard deviation of the ISIs distribution. Ranging between ± 1, B indicates to which degree the temporal regime of a process exhibits a poissonian (B$\cong$0), periodic (B$\cong$-1) or bursty (B$\cong$1) behaviour.

We also computed the memory coefficient (M) defined as:

$$M = \frac{1}{n-1} \sum_{i=1}^{n-1} \frac{\langle \tau_i \tau_{i+1} \rangle - \langle \tau_i \rangle \langle \tau_{i+1} \rangle}{\sigma_i \sigma_{i+1}}$$

M is a correlation-based measure defined as a linear (Pearson) correlation coeficient between ISIs and the interevent time between two consecutive saccades (ISI+1) where n is the total number of ISIs and $\langle \tau_{i+1} \rangle$ and σ_{i+1} are the mean and standard deviation of the ISI+1 respectively. This quantity also ranges between ± 1 M indicating the role of memory in the emergence of a poissonian (M$\cong$0), periodic (M$\cong$-1) or bursty (M$\cong$1) temporal dynamics expressing the tendency of ISIs being followed by similar or discrepant size ISIs. For

mapping mechanisms leading to the observed temporal regime, the effect of B and M were illustrated by placing saccades sequences in a diagram called the B-M plane.

Statistical analyses

To determine significant inter-species differences in B and M variables we used pairwise (t-tests). In all tests, the significant level was $P < 0.05$. Measurements are presented as the arithmetic mean ± SEM. Statistical analyses were conducted with JMP®, (SAS Institute Inc., Cary, NC, 1989–2021).

RESULTS

A wide range of behavioural categories was identified in the video analyses and categorized into three groups (Fig. 1). Saccade occurrences were distributed throughout the recording period and were the most frequently observed behaviour (mean = 1 409 ± 189 ms) at a mean rate of 0.39 ± 0.05 Hz and with a mean ISI duration of 2 690 ± 360 ms. Given that the animals were unrestricted in their movements, they occasionally exhibited other forms of visuomotor behaviours not identified as saccadic gaze shifts such as peering, smooth pursuit and blink and behaviours that did not require active engagement in visual search such as locomotion, maintenance and drowsiness.
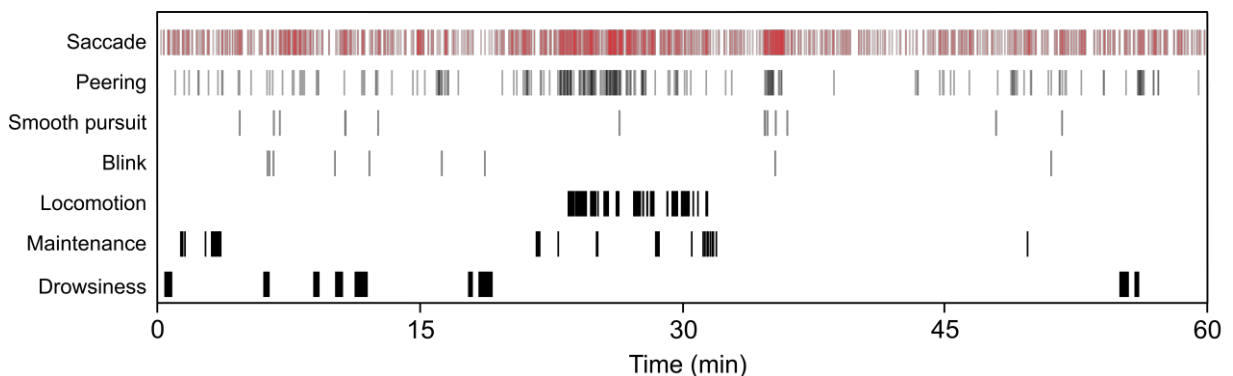
Figure 1. Distribution of behavioural occurrences across one representative video recording of a Ferruginous pygmy owl (subject GB1902). Saccade occurrences are represented by red dashes; occurrence of other forms of visuomotor behaviour are represented in grey; occurrence of behaviours not directly related to visual search are represented in black.

Therefore the first step in characterizing the saccade temporal dynamics was carried out by calculating the ISR. Varying from 0,018 Hz to 12,5 Hz throughout the one-hour recordings, when plotted against time the instantaneous saccade rate revealed a temporal regime with short bouts of increased activity rate interspaced by longer periods of reduced activity rate (Fig. 2).
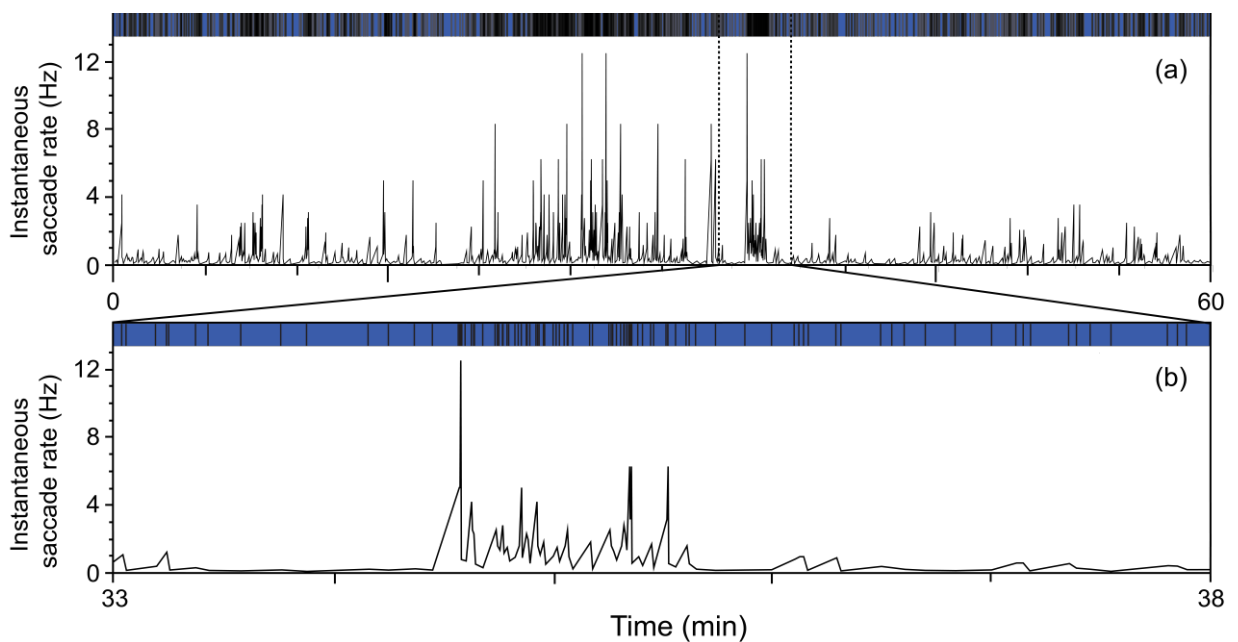
Figure 2. GB1902 saccade time series and ISR. (a-b) Saccade occurrences are represented by black dashes; ISIs are represented by blue rectangles between saccades; ISR is represented directly above

associated saccade sequences. (a) Complete one-hour representative recording (subject GB1902). (b) Five minutes section of the same recording.

The ISI probability distribution of the four subjects followed a positively skewed, heavy-tailed profile suggesting that in this avian species saccades are generated by a mechanism that can not be explained as a homogeneous process (Fig. 3). In rare events (0.7%) there were indications of ISIs with less than 80 ms between head saccades indicating that if a fixation occurred in this period it was probably shorter.
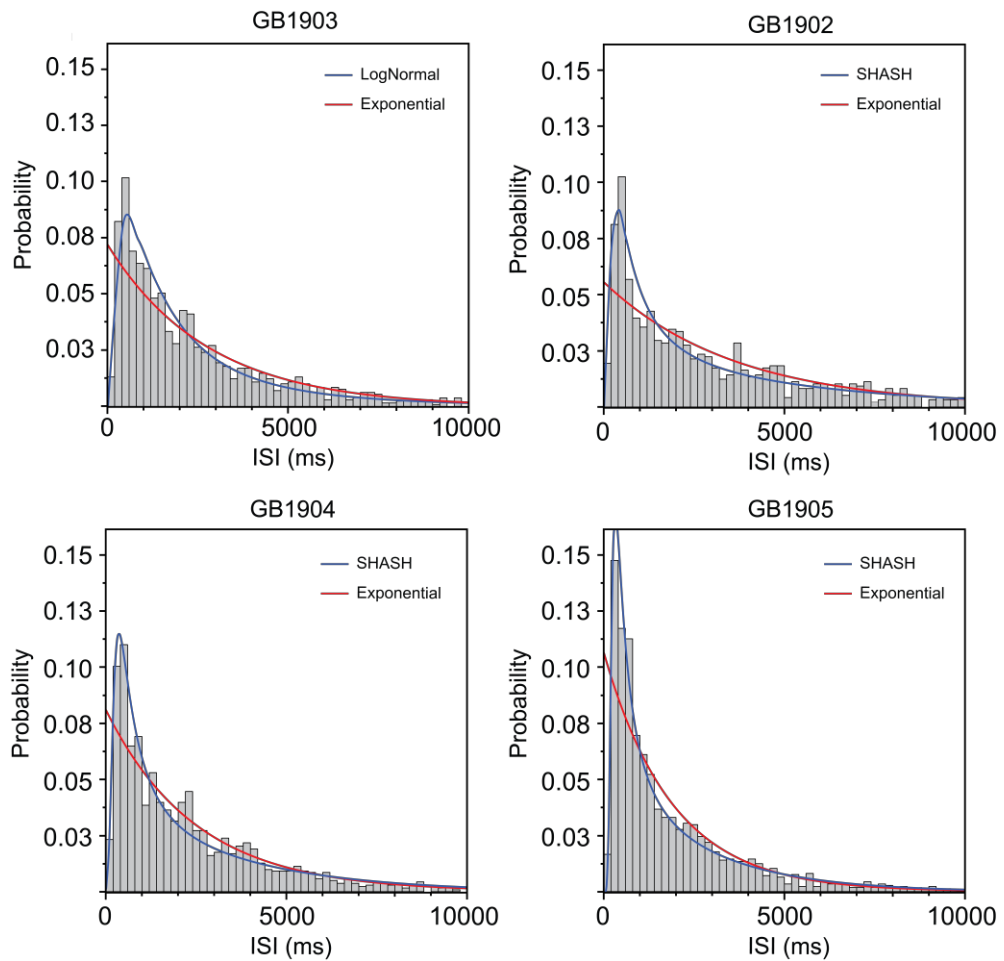
Figure 3. ISI probability distribution of single-subject saccade sequences. The Poissonian fitted model is represented by the exponentially decaying line in red. The best-fitted model in the ΔAIC selection is represented by the blue line. In the subject GB1903 pannel, the blue line represents a log-normal fitted distribution. For the other three subjects, the blue line represents the fitted SHASH distribution.

Among the four models considered here, the best one in subjects GB1902, GB1904 and GB1905 were SHASH. Only subject GB1903 presented a log-normal relative best fit. Except for SHASH in GB1902, the relative performance of every fitted model expressed by the ΔAIC P-value were below the acceptable (0.05) for inferring a god fit (Table 2).

Table 2. Model selection results.

Analysis	Variable	Owl			
		GB1902	GB1903	GB1904	GB1905
Sample size	n	994	1294	1440	1902
Mean rate (Hz)		0.28	0.36	0.4	0.53
Model *Δ*AIC (Goodness of fit *P*-value)	Exponential	91.60 (<0.01)	196.35 (<0.01)	106.55 (<0.01)	364.65 (<0.01)
	Log normal	65.70 (<0.01)	**0** (<0.01)	12.17 (<0.01)	97.04 (<0.01)
	Weibull	87.40 (<0.01)	193.36 (<0.01)	108.56 (<0.01)	364.90 (<0.01)
	SHASH	**0** **(0.059)**	55.0 (<0.0001)	**0** (<0.0001)	**0** (<0.0011)

[1] Model ΔAIC P-value of relative best-fitted models are shown in bold.

In line with the ISIs heavy-tail distribution and its divergence from the exponential model evidenced by our model selection analysis, values of the burstiness index and memory coefficient were positive (Fig. 4), indicating that Ferruginous pygmy owl saccades follow a bursty temporal pattern. Comparing B and M obtained in this species with the ones from burrowing owls (n = 6, *Athene cunicularia*) 24-hour saccade datasets obtained from a previous study (Baron, unpublished data), we found a significantly higher B ($t_{6.6} = 9.7$, P = 0.0001) and a slightly higher but is still statistically different M ($t_7 = 3.0$, P = 0.0174). The burrowing owl saccade signals were extracted using essentially the same experimental and video analyses procedures described in methods but with a temporal resolution of 1 second.
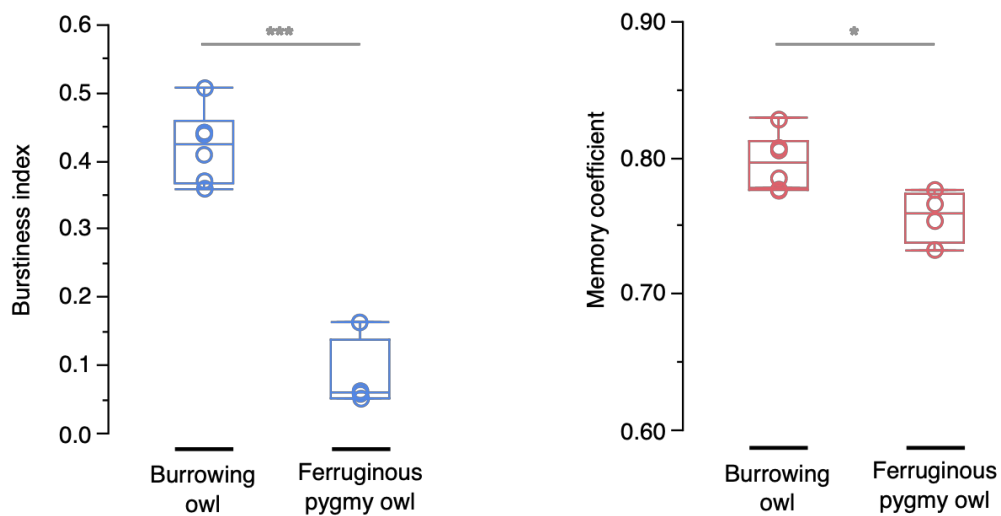
Figure 4. Comparison between the Burstiness index (blue) and the Memory coefficient (red) of two owl species.

Using data from a human-saccade database of subjects (n = 5) free viewing videos of natural scenes (Dorr 2010) and one marmoset saccade data sample we extended our analyses

to primates. When comparing Ferruginous pygmy owls with human subjects there was no significant difference in B ($t_{6.9}$ = -0.03, P = 0.9) and mild significant difference in M ($t_{6.9}$ = -2.91, P = 0.02) was found. In contrast, when compared to humans the burrowing owl presented a B significantly higher ($t_{7.1}$ = -6.2, P = 0.0002) and also a M slightly higher ($t_{6.3}$ = -4.6, P = 0.0016). By adopting the representation in the B-M plane we compared tendencies in saccade temporal dynamics (fig. 5).
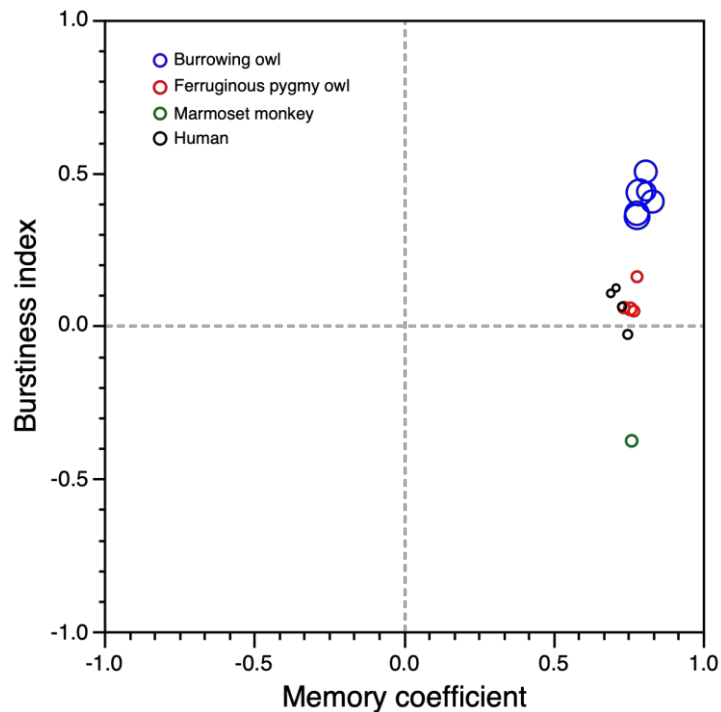
Figure 5. Saccade sequences of four different species represented in the B-M plane. Circles scale relates to saccade sample size. Ferruginous pygmy owl (red); Burrowing owl (blue); Black-tufted marmoset (green); human subjects (black).

DISCUSSION

Our findings indicate that Ferruginous pygmy owl saccadic gaze shift rate has higher when compared to other owl species. Barn owls in a controlled free-view experimental context exhibited 0.32 Hz (Harmening et al., 2011) and burrowing owls in similar naturalistic conditions to ones provided by this study presented a 0.16 Hz saccade rate (Baron, unpublished data). To prevent loss in therms of behavioural richness, in this study the animals were filmed from a "third-person" viewpoint. This approach permitted observations without great interventions. In that way, the animals displayed a wide range of behavioural categories, which may not be possible in a more restrained experimental setting.

Different data acquisition approaches can be a fator of variation in saccade rates. Nonetheless, the observed higher frequency may also be a result of the ecological constraints encountered by Ferruginous pygmy owls in the wild. This bird is one of the smallest owl species in the world with about 12 centimetres long from head to tail and weighing no more than 90 grams. The presence of symmetrical ears also indicates great dependence on vision in acquiring food and escaping from predators (Proudfoot et al., 1999). Altogether these factors may have led to adaptations related to the need for a more recurrent visual sampling of the environment.

In comparison to other bird representants, the Ferruginous pygmy owl also displayed a relatively high head-saccade rate. Under captive conditions, raptors like the Copper's hank (*Accipiter cooperii)* present an approximately 1 Hz followed by the American kestrel (*Falco sparverius*) and the Red-tailed hawk (*Buteo jamaicensis*) with approximately 0.4 Hz mean head saccade frequencies (O'Rourke et al., 2010). These are among the highest observed in birds. In terms of mean ISI duration we have in one extreme the Copper's hank and the Indian peafowl (*Pavo cristatus*) presenting approximately 1 second (s) (O'Rourke et al., 2010; Wallman & Pettigrew, 1985; Yorzinski et al., 2015) and in the other, the Tawny frogmouth (*Podargus strigoides*) with up to 40 s respectively (O'Rourke et al., 2010; Wallman &

Pettigrew, 1985; Yorzinski et al., 2015). The Ferruginous pygmy owl presents a middle term mean ISI duration that more closely resembles Little eagle's (*Hieraaetus morphnoides*) 2.5 s duration (Wallman & Pettigrew, 1985). It is important to highlight that in natural conditions all these species also engage in eye saccades during visual search. This adds more complexity to this behaviour making predictions about the luminance pattern in which the retina of these animals will be exposed more difficult.

Despite more than 200 million years of evolutionary divergence owls present similarities with primates in terms of visual perception (Baron 2007, Pinto 2009, Ohayon 2006). Humans and non-human primates present varying saccade rates depending on task demands (Chen et al., 2021; Mitchell et al., 2014). By analysing eye saccade time series of human subjects watching naturalistic videos we found a 1.3 Hz rate. The high M score found in human subjects is consistent with the idea of a short term memory-driven mechanism generating saccades (Amit et al., 2017a). Admitting we used data from one single Black-tufted marmoset, the B and M obtained in this subject saccade sequence lead to infer some degree of regularity in the saccade temporal pattern in this species.

The existence of a post-saccadic "refractory period" in owls is still unknown. A low probability of ISIs with less than 160 ms found in our data may suggest its presence. To estimate post saccadic inhibition a visual saliency related experimental approach could be used (Harris, 1989) since saliency based on orientation has been previously demonstrated in owls (Ohayon, 2006).

The AIC selection results show that none of the four considered models satisfactorily fitted with our data meaning they could not capture the Ferruginous pygmy owl ISI distribution. As expected, admitting the fluctuation in saccade rate evidenced by the ISR the exponential (poissonian) model performed badly indicating saccade occurrences are not independent of each other. Within the four ranked distribution functions, the Weibull

performed the worst. Considering its capacity to describe human saccade first-order dependencies (Harris, 1989) and the high M score found in the Ferruginous pygmy owl data, this result suggests that the dependence between saccade occurrences in this avian species may be determined by a mechanism not captured by this model. It is important to highlight the distinct experimental approaches in which the saccades were scored in both studies, although is possible that this could as well be the effect of a longer owl post-saccadic "refractory period". The relative preference for the SHASH model was expected as visual inspection of the data indicated the presence of heavy tails in the ISI distributions what is consistent with a bursty temporal dynamics (Goh & Barabási, 2008).

When investigating human eye-saccade temporal dynamics, Amit and colleagues (Amit et al., 2017) found that the rhythmicity of saccades could parsimoniously be explained by first-order statistical dependencies in opposition to an oscillatory process. This suggests that this rhythm is mainly dictated by the strong correlation between consecutive saccade occurrences. Without the evident influence of periodic cortical oscillations, the author argued that saccades themselves are critical for injecting rhythmicity into the neural system. Likewise, the methodology adopted to characterize the dynamical proprieties of saccades in this study is capable of identifying the possible first-order dependences in temporal patterns by quantifying the memory effect. This is accomplished by comparing the magnitude of B and M quantitative estimates on the emergence of a bursty dynamics (Goh & Barabási, 2008).

Our results evidenced a strong memory effect in Ferruginous pygmy owls and humans. Contrastingly, based on the high B score, in burrowing owls the ISI variability is also a strong factor determining a bursty saccade temporal dynamics. It is also interesting to note the similar M values in all groups. This could indicate a concerved mechanism driving saccade rhythm, or even another evolutionary convergence between owls and primates? This

issue is not close to be resolved and deserves a more profound analysis. Extending this investigation to other animal groups including invertebrates could help clarify this question.

Decades ago, Yarbus pioneer work evidenced the link between higher cognitive processes and visual search. Even today, his work profoundly impacts research on visuomotor behaviour (Tatler et al., 2010). A growing number of studies are aimed at associating alterations in saccade patterns with several mental illnesses even in prodromic phases (Morita et al., 2019; Yang et al., 2013). Using eye-tracking techniques Carr (2020) demonstrated the possibility of also assessing elderly driver safety. What if examining saccades in the temporal dimension could also lead to a more precise detection of cognitive disabilities? The method described in this study is suitable for detecting discrepancies in saccade temporal dynamics. Whether it could be applied to assess mental health should be addressed in future studies.

REFERENCES

Akaike, H. (1974). A new look at the statistical model identification. *IEEE Transactions on Automatic Control*, *19*(6), 716–723. https://doi.org/10.1109/tac.1974.1100705

Amit, R., Abeles, D., Bar-Gad, I., & Yuval-Greenberg, S. (2017). Temporal dynamics of saccades explained by a self-paced process. *Scientific Reports*, *7*(1), 886. https://doi.org/10.1038/s41598-017-00881-7

Baron, J., Pinto, L., Dias, M. O., Lima, B., & Neuenschwander, S. (2007). Directional responses of visual wulst neurones to grating and plaid patterns in the awake owl. *European Journal of Neuroscience*, *26*(7), 1950–1968. https://doi.org/10.1111/j.1460-9568.2007.05783.x

Baudot, P., Levy, M., Marre, O., Monier, C., Pananceau, M., & Frégnac, Y. (2013).

Animation of natural scene by virtual eye-movements evokes high precision and low noise in V1 neurons. *Frontiers in Neural Circuits*, *7*, 206. https://doi.org/10.3389/fncir.2013.00206

Burnham, K. P., & Anderson, D. R. (2002). *Model Selection and Multimodel Inference, A Practical Information-Theoretic Approach*. https://doi.org/10.1007/978-0-387-22456-5_5

Carr, D. B., & Grover, P. (2020). The Role of Eye Tracking Technology in Assessing Older Driver Safety. *Geriatrics*, *5*(2), 36. https://doi.org/10.3390/geriatrics5020036

Cartron, J.-L. E., & Finch, D. M. (2000). Ecology and conservation of the cactus ferruginous pygmy-owl in Arizona. *Gen. Tech. Rep. RMRS-GTR-43. Ogden, UT: U.S. Department of Agriculture, Forest Service, Rocky Mountain Research Station. 68 p.*, *043*. https://doi.org/10.2737/rmrs-gtr-43

Chen, C.-Y., Matrov, D., Veale, R., Onoe, H., Yoshida, M., Miura, K., & Isa, T. (2021). Properties of visually guided saccadic behavior and bottom-up attention in marmoset, macaque, and human. *Journal of Neurophysiology*, *125*(2), 437–457. https://doi.org/10.1152/jn.00312.2020

Dorr, M., Martinetz, T., Gegenfurtner, K. R., & Barth, E. (2010). Variability of eye movements when viewing dynamic natural scenes. *Journal of Vision*, *10*(10), 28–28. https://doi.org/10.1167/10.10.28

Goh, K.-I., & Barabási, A.-L. (2008). Burstiness and memory in complex systems. *EPL*, *81*(4), 48002. https://doi.org/10.*1*209/0295-5075/81/48002

Harmening, W. M., Orlowski, J., Ben-Shahar, O., & Wagner, H. (2011). Overt attention toward oriented objects in free-viewing barn owls. *Proceedings of the National Academy of Sciences*, *108*(20), 8461–8466. https://doi.org/10.1073/pnas.1101582108

Harris, C. M. (1989). The ethology of saccades: a non-cognitive model. *Biological Cybernetics*, *60*(6), 401–410. https://doi.org/10.1007/bf00204695

Hayhoe, M., & Ballard, D. (2005). Eye movements in natural behavior. *Trends in Cognitive*

Sciences, *9*(4), 188–194. https://doi.org/10.1016/j.tics.2005.02.009

Jones, M. C., & Pewsey, A. (2009). Sinh-arcsinh distributions. *Biometrika*, *96*(4), 761–780. https://doi.org/10.1093/biomet/asp053

Land, M. (2019). Eye movements in man and other animals. *Vision Research*, *162*, 1–7. https://doi.org/10.1016/j.visres.2019.06.004

Land, M. F. (1999). Motion and vision: why animals move their eyes. *Journal of Comparative Physiology A*, *185*(4), *3*41–352. https://doi.org/10.1007/s003590050393

Land, M. F. (*2015*). Eye movements of vertebrates and their relation to eye form and function. Journal of Comparative Physiology A, 201(2), 195–214. https://doi.org/10.1007/s00359-014-0964-5

Mitchell, J. F., Reynolds, J. H., & Miller, C. T. (2014). Active Vision in Marmosets: A Model System for Visual Neuroscience. Journal of Neuroscience, 34(4), 1183–1194. https://doi.org/10.1523/jneurosci.3899-13.2014

Morita, K., Miura, K., Kasai, K., & Hashimoto, R. (2019). Eye movement characteristics in schizophrenia: A recent update with clinical implications. *Neuropsychopharmacology Reports*, *40*(1), 2–9. https://doi.org/10.1002/npr2.12087

Motta-Junior, J. C. (2007). Ferruginous Pygmy-owl (Glaucidium brasilianum) predation on a mobbing Fork-tailed Flycatcher (Tyrannus savana) in south-east Brazil. *Biota Neotropica*, *7*(2), 0–0. https://doi.org/10.1590/s1676-06032007000200038

Ohayon, S., Willigen, R. F. van der, Wagner, H., Katsman, I., & Rivlin, E. (2006). On the barn owl's visual pre-attack behavior: I. Structure of head movements and motion patterns. Journal of Comparative Physiology A, *192*(9), 927–940. https://doi.org/10.1007/s00359-006-01*30*-9

O'Rourke, C. T., Pitlik, T., Hoover, M., & Fernández-Juricic, E. (2010). Hawk Eyes II: Diurnal Raptors Differ in Head Movement Strategies When Scanning from Perches. *PLoS*

ONE, *5*(9), e12169. https://doi.org/10.1371/journal.pone.0012169

Pinto, L., & Baron, J. (2009). Spatiotemporal frequency and speed tuning in the owl visual wulst. European Journal of Neuroscience, 30(7), 1251–1268. https://doi.org/10.1111/j.1460-9568.2009.06918.x

Proudfoot, G. A., (deceased), S. L. B., & Chavez-Ramirez, and F. (1999). *Biology of Ferruginous Pygmy-Owls in Texas and Application of Artificial Nest Structures*.

Sarasola, J. H., & Santillán, M. Á. (2014). Spatial and temporal variations in the feeding ecology of ferruginous pygmy-owls (Glaucidium brasilianum) in semiarid forests of central Argentina. *Journal of Arid Environments*, *109*, 39–43. https://doi.org/10.1016/j.jaridenv.2014.05.008

Sazima, I. (2015). Lightning predator: the Ferruginous Pygmy Owl snatches flower-visiting hummingbirds in southwestern Brazil. *Revista Brasileira de Ornitologia*, *23*(1), 12–14. https://doi.org/10.1007/bf03544283

Tatler, B. W., Wade, N. J., Kwan, H., Findlay, J. M., & Velichkovsky, B. M. (2010). Yarbus, Eye Movements, and Vision. *I-Perception*, *1*(1), 7–27. https://doi.org/10.1068/i0382

Wagner, H., Kettler, L., Orlowski, J., & Tellers, P. (2013). Neuroethology of prey capture in the barn owl (Tyto alba L.). *Journal of Physiology-Paris*, *107*(1–2), 51–61. https://doi.org/10.1016/j.jphysparis.2012.03.004

Wallman, J., & Pettigrew, J. (1985). Conjugate and disjunctive saccades in two avian species with contrasting oculomotor strategies. *The Journal of Neuroscience*, *5*(6), 1418–1428. https://doi.org/10.1523/jneurosci.05-06-01418.1985

Wang, H. X., Freeman, J., Merriam, E. P., Hasson, U., & Heeger, D. J. (2012). Temporal eye movement strategies during naturalistic viewing. Journal of Vision, 12(1), 16–16. https://doi.org/10.1167/12.1.16

Yang, Q., Wang, T., Su, N., Xiao, S., & Kapoula, Z. (2013). Specific saccade deficits in

patients with Alzheimer's disease at mild to moderate stage and in patients with amnestic

mild cognitive impairment. *AGE*, *35*(4), 1287–1298. https://doi.org/10.1007/s11357-012-

9420-z

Yorzinski, J. L., Patricelli, G. L., Platt, M. L., & Land, M. F. (2015). Eye and head

movements shape gaze shifts in Indian peafowl. *Journal of Experimental Biology*, *218*(23),

3771–3776. https://doi.org/10.1242/jeb.129544